HHS Public Access

Author manuscript

Auton Neurosci. Author manuscript; available in PMC 2018 November 01.

Published in final edited form as:

Auton Neurosci. 2017 November ; 207: 48–58. doi:10.1016/j.autneu.2017.07.008.

Cardiac neuroanatomy - Imaging nerves to define functional control

Peter Hanna[1], **Pradeep S. Rajendran**[1,2], **Olujimi A. Ajijola**[1], **Marmar Vaseghi**[1], **J. Andrew Armour**[1], **Jefrrey L. Ardell**[1,2], and **Kalyanam Shivkumar**[1,2]

[1]University of California Los Angeles (UCLA) Cardiac Arrhythmia Center and Neurocardiology Research Center of Excellence, David Geffen School of Medicine, UCLA, Los Angeles, CA, USA

[2]Molecular, Cellular & Integrative Physiology Program, David Geffen School of Medicine, UCLA, Los Angeles, CA, USA

Abstract

The autonomic nervous system regulates normal cardiovascular function and plays a critical role in the pathophysiology of cardiovascular disease. Further understanding of the interplay between the autonomic nervous and cardiovascular systems holds promise for the development of neuroscience-based cardiovascular therapeutics. To this end, techniques to image myocardial innervation will help provide a basis for understanding the fundamental underpinnings of cardiac neural control. In this review, we detail the evolution of gross and microscopic anatomical studies for functional mapping of cardiac neuroanatomy.

Keywords

neurocardiology; intracardic nervous system; myocardial innervation; autonomic nervous system

INTRODUCTION

The autonomic nervous system (ANS) enables integrative control of the viscera to ensure survival of the organism.[1] Specifically, the cardiac ANS plays a crucial role to maintain normal rhythm and sustain the circulation of blood. The cardiac ANS intricately regulates all the critical physiological functions of the heart (chronotropy, dromotropy, inotropy, and lusitropy). The interplay of the ANS and the heart is readily apparent in the pathophysiology of most cardiovascular diseases including hypertension, heart failure, myocardial infarction and arrhythmias.[2–6] The study of such interactions has led to the development of neuromodulatory therapies that treat cardiac disease, ranging from vagus nerve stimulation to bilateral cardiac sympathetic decentralization for heart failure and ventricular arrhythmias.[7–9] A more thorough characterization of cardiac innervation will promote

Address correspondence to: Kalyanam Shivkumar, MD PhD, UCLA Cardiac Arrhythmia Center, 100 UCLA Medical Plaza, Suite 660, Los Angeles, CA 90095, Phone: 310-206-6433, kshivkumar@mednet.ucla.edu.

further study of neural control of cardiac function and allow for the development of targeted cardiovascular therapeutics.[10] In this review, we describe available and burgeoning techniques in mapping the structure and function of cardiac neuroanatomy.

Functional organization of the cardiac nervous system

Anatomically, cardiac nerves are complex, and detailed atlases of cardiac innervation are few in number (Figures 1–3). Macroscopic images of cardiac nerves depicted in anatomical texts since the late 1500s are reproduced in books and anatomical studies without histological confirmation of whether structures labeled as 'nerves' are actually neural. Indeed, when neural structures are surgically targeted for therapeutics in clinical care (e.g. bilateral cardiac sympathetic decentralization), intra-operative histological confirmation is sought to confirm that neural tissue was indeed removed.[11] The problem at the level of the heart is compounded by the lack of technology for high-resolution microscopic studies until very recently. Furthermore, methods to handle the very large image datasets and the bioinformatics tools for neuronal tracing in images and three-dimensional reconstruction have only recently been developed. Placing these images in their functional context, using state-of-the-art physiological approaches from micro-stimulation to neural recordings, are required for interpretation of normal physiology. Finally, integrating anatomical and functional data would provide the framework needed to precisely define the changes in innervation due to disease (neural remodeling) and assure correct utilization and monitoring of new or pre-existing methods for neuromodulation.

Gross anatomy of neurotransmission to and from the heart

The gross anatomy of cardiac innervation has been the subject of investigation for a number of years. Dissections of mammals and human cadavers have illustrated that myocardial innervation is conserved to a significant degree among species.[12–18] The ANS innervating the heart has been categorized into: i) central; ii) intrathoracic extra-cardiac; and iii) intrinsic cardiac components (Figures 1–3). The intrathoracic extrinsic cardiac nervous system connects the intrinsic cardiac nervous system within the heart to the central nervous system. It is composed of parasympathetic and sympathetic motor components that exert opposing effects on cardiac electrical and mechanical indices.

Parasympathetic motor neurons—Preganglionic neurons of the parasympathetic nervous system are located in the nucleus ambiguus and dorsal motor nucleus of the medulla oblongata as well as scattered regions in between these two structures.[19,20] These project axons via the vagus nerve and its multiple intrathoracic cardiopulmonary branches to efferent postganglionic parasympathetic neurons in the numerous intrinsic cardiac ganglia.[21] Postganglionic efferent parasympathetic neurons located in individual cardiac ganglia receive preganglionic inputs from both the right and left vagal trunks.[22] Anatomic dissections in canines have demonstrated that postganglionic vagal neurons to the sinoatrial (SA) node are found predominantly in a ganglionated plexus next to the right pulmonary vein-atrial junction, while the postganglionic vagal neurons that influence the atrioventricular (AV) node are located predominantly in the region adjacent to the inferior vena cava-inferior left atrium junction.[23]

Sympathetic motor neurons—Sympathetic efferent preganglionic neurons originate in the intermediolateral cell column of the spinal cord and project via C7-T6 rami to postganglionic sympathetic neurons in the superior cervical, middle cervical, cervicothoracic (stellate) ganglia (sympathetic chain), and mediastinal ganglia.[16,18] These postganglionic neurons project axons via multiple cardiopulmonary nerves to atrial and ventricular myocardium and limited populations of intrinsic cardiac adrenergic neurons. Kawashima published a detailed study in 2005 that analyzed the origin and course of the autonomic nerves in human cadavers using microscopy, highlighting the conserved nature of the superior and middle cervical, mediastinal, and stellate ganglia across species.[18]

Sensory neurons—Cardiac afferents provide beat-to-beat sensory information of cardiac function and microenvironment to the neuraxis, and additional information is conveyed by arterial mechano-and chemoreceptors (Figure 2). Afferent nerves travel within the vagal trunk and ‘sympathetic’ fibers to the nodose and dorsal root ganglia, respectively. The processing of afferent information at multiple levels, including the intrinsic cardiac nervous system, extracardiac intrathoracic ganglia, spinal cord, brain stem, and higher centers, provides an elegant mechanism of interacting feedback loops that modulate efferent cardiomotor (sympathetic and parasympathetic) signals for maintaining normal rhythm and life-sustaining circulation.

The intrinsic cardiac nervous system—In contrast to the extrinsic components of the ANS, intrinsic cardiac neurons are found in intramural ganglia and in epicardial fat pads that obscure direct visualization (Figure 4).[24,25] While these neuronal somata were identified early in the last century, the location and connections of these neurons have remained poorly understood.[26] Subsequent study using light and electron microscopy confirmed these structures in the human heart (Figures 4C–E).[25] It is now known that the intrinsic cardiac ganglionated plexuses contain complex networks of neurons and interconnecting nerves that include the following subtypes: i) afferent neurons; ii) motor (parasympathetic and sympathetic) neurons; and iii) interconnecting local circuit neurons.[27] Taken together, this neural network at the level of the heart is thought to play an important role in modulating cardio-cardiac reflexes.

Histochemical and immunohistochemical techniques

Histochemical techniques have characterized the richness of myocardial innervation. Cresyl violet staining has been used to identify the cytoplasmic Nissl substance in autonomic neurons.[17,24,28] The retrograde transport of horseradish peroxidase and vital dyes applied to various cardiac tissues had been used to identify the locations of cardiac vagal preganglionic neurons in the medulla.[29,30] This technique has helped characterize the locations of sympathetic postganglionic neuronal somata and vagal preganglionic efferent neurons innervating feline and canine hearts.[16] This marker has also proved helpful in delineating locations of afferent neurons in nodose and dorsal root ganglia that transduce the mechanical and/or chemical milieu of various regions of the heart or great vessels to the nervous system.[31–33] Xrhodamine-5-(and 6)-isothiocyanate (XRITC) is another marker that serves as a retrograde fluorescent tracer for preganglionic vagal neurons.[34,35] As mentioned above, visualization of the intrinsic cardiac nervous system has proved challenging, and fluorescent

dyes, Fast Blue and bisbenzimide, have been used to demonstrate retrograde transport that confirm the presence of interneuronal connections.[36–38] Antibodies against cholera toxin subunit B have also been used in immunohistochemical studies of the intracardiac ganglia.[39]

Specific identification of neuron types in the two limbs of the ANS is made possible by targeting select neurotransmitters associated with sympathetic or parasympathetic neuronal somata located in the peripheral cardiac ANS. Postganglionic parasympathetic neurons utilize the neurotransmitter acetylcholine, degraded by the enzyme acetylcholinesterase selectively associated with parasympathetic motor neurons. As such, many studies use acetylcholine to mimic the effects of vagal stimulation.[40,41] Karnovsky and Roots published a histochemical method in 1964 that utilized a thiocholine ester that is hydrolyzed by cholinesterase to form copper thiocholine, which appears brown when treated with ammonium sulfide.[42] This method and refinements of this method including, but not limited to, the use of acetylthiocholine and the use of a marker of the peroxidase activity of the reaction product have been used to study the distribution of cholinergic neurons in the heart (Figure 5).[43–49] For example, Pauza et al. showed that the number of intrinsic cholinergic neurons in the heart was directly proportional to ganglia area in guinea pig, rat, dog, and human hearts using such methods.[48,50,51]

While this histologic method identifies cholinesterase activity associated with select populations of neuronal somata, it is not specific for acetylcholinesterase activity in vagal neurons. As such, immunohistochemcial methods have been used to identify parasympathetic neurons using antibodies against choline acetyltransferase (ChAT, Figure 5A–C). This methodology was initially utilized in the characterization of guinea pig myenteric plexus neurons associated with the gastrointestinal tract.[52] It was thereafter applied to study of guinea pig cardiac ganglia and is now in widespread use.[53,54] Additional markers such as choline transporter and vesicular acetylcholine transporter, which are more specific for the identification cholinergic neurons, have since been developed.[55,56]

Similarly, sympathetic neurons can be identified using immunohistochemcial markers that target an enzyme specific to these neurons. With respect to adrenergic neurons, tyrosine hydroxylase (TH) is the enzyme involved in the rate-limiting step in norepinephrine synthesis and, as such, is specific for norepinephrine-producing neurons (Figure 5D–F). Pickel et al. developed antibodies against TH that performed well for localization of neurons involved in biosynthesis of catecholamines.[28] Immunohistochemistry targeting of TH has been used regularly to characterize the sympathetic innervation of the heart across different animal models.[45,49,53,57,58] Pan-neuronal markers are used to identify cardiac nerves, and examples include the neurofilament markers β-tubulin III and protein gene product 9.5 that are found almost exclusively in neurons (Figure 6).[45,50,56,57,59–62] Presynaptic nerves are targeted using antibodies against synapsin I, which is a member of a family of neuron-specific proteins that interact with synaptic vesicles.[61,63]

While the majority of these intracardiac neurons are either parasympathetic or sympathetic in nature, intracardiac nerves are not exclusively parasympathetic or sympathetic. Thus, the use of additional markers has helped elucidate the mixed cholinergic and adrenergic phenotype of intrinsic cardiac neurons and nerves in the heart. For example, Hoard et al.

demonstrated the presence of cholinergic neurons in intrinsic cardiac ganglia that are associated with tyrosine hydroxylase, dopamine β-hydroxylase, and norepinephrine transporter, yet do not contain vesicular monoamine transporter type 2 (VMAT2) and thereby precludes the ability to store norepinephrine.[62] Rysevaite et al. showed that 83% of intrinsic cardiac neurons were ChAT immunoreactive, 4% were TH immunoreactive, and 14% were immunoreactive for both ChAT and TH.[64] This study also demonstrated immunoreactivity to calcitonin gene-related peptide and substance P, neuropeptides found in nociceptive neurons, to identify a population of afferent neurons in the intrinsic cardiac nervous system.[64]

Antibody-based approaches have inherent limitations with respect to fidelity of results. In that regard, the use of transgenic mice has allowed for a more detailed structural analysis, as in the morphogenesis of the cardiac nervous system. In mouse studies, wingless type integration site family, member 1 (Wnt1)-Cre recombinase (Cre) mice have been used to identify tissues derived from neural crest cells, as *Wnt1* is only expressed during embryonic development of the central nervous system.[65] White et al. demonstrated that crossing these mice with mice expressing the tdTomato reporter results in neural crest-derived cells that are labeled with red fluorescence and imaged using epifluorescent stereomicroscopy to image the subepicardial neural network in exquisite detail.[61]

Mapping the fine neural network across large distances in organs has typically been performed using histological sections that are then reconstructed, a time-consuming process that also suffers from loss in fidelity due to tissue distortion. Light scatter due to tissue inhomogeneity has hindered imaging larger volumes of tissue. Tissue clearing approaches, initially developed to better visualize neural networks in the central nervous system, attempt to minimize light scatter by decreasing tissue inhomogeneity and allowing for deeper imaging in thick sections or intact tissues while preserving the three-dimensional molecular and cellular architecture. Two main subgroups of techniques include solvent-based methods, such as BABB,[66] tetrahydrofuran and dibenzylether,[67] 3DISCO[68] and iDISCO, or aqueous-based methods, including Sca*l*e, SeeDB, CUBIC, *Clear*^{T}, *Clear*^{T2}, CLARITY, and PACT, are used to remove the lipid membranes of cells, which are the major source of tissue heterogeneity and, hence, light diffraction, to generate optically transparent tissue.[67–75] While various challenges face these differing techniques including time intensity, degree of tissue clearing, preservation of fluorescence of reporters, and tissue expansion, the rapidly evolving field holds the promise of improved three-dimensional imaging at depth. In conjunction with these developments, advances in microscopy in the form of laser-scanning confocal, two-photon, and light-sheet microscopy permit volumetric imaging of cleared tissues. The premise of these techniques is to image discrete planes within a volume and minimize out-of-focus light to yield improved imaging at depth.

Functional mapping

Given the complex structure of parasympathetic, sympathetic motor and other intrinsic cardiac neurons within the heart, mapping studies have been performed to elucidate the functional architecture of the cardiac nervous system. Studies have evaluated how autonomic nerve stimulation affects mechanical and electrocardiographic parameters of the heart

(Figure 7).[76–79] Norris et al. placed strain gauges on the epicardium and electrically stimulated sympathetic nerves in canines to measure regional inotropy to determine gross functional innervation patterns.[80,81] The positive and negative chronotropic effect of sympathetic and parasympathetic simulation on SA node activity, respectively, were originally described in studies employing nerve stimulation while monitoring heart rate. These studies determine that the right vagus nerve primarily affecting the SA node while the left vagus nerve exerted predominant influence on the AV node in the canine heart.[82,83] Randall et al. demonstrated that parasympathetic stimulation resulted in decreased chronotropy and decreased AV conduction, while Loeb and DeTarnowsky showed how sympathetic nerve stimulation resulted in increased AV conduction through the use of intracardiac electrograms in *in vivo* experiments in dog.[84,85] More recently, a model of isolated Langendorff rabbit heart with intact dual autonomic innervation has allowed for *in vitro* preparations that are devoid of confounding neurohormonal influences of *in vivo* models.[86]

Optogenetic Techniques

In contrast to optical mapping, which is helpful at the organ level, optogenetics provide functional information on myocardial innervation at the cellular level. Optogenetic methods utilize light-activated ion channels called opsins to activate or inhibit specific cell types such as neural populations *in vivo*, providing spatiotemporal resolution in unprecedented detail and allowing the study of structure and function.

The application of optogenetics in neurons was developed over a decade ago and has since been translated to the study in neurocardiology.[87–89] Channelrhodopsin 2 (ChR2) is an opsin, or light-gated ion channel, identified in unicellular green alga *Chlamydomonas reinhardtii*.[88] When ChR2 is expressed in a neuron, inward currents are evoked within 50ms of a flash of blue light, and this technology has be used for fast neuronal photostimulation in mammals.[89] Improvements of this tool include ChR2 variants that increase the magnitude of photocurrents induced.[90–92] In the brain, multidiode probe arrays have been used in studies of local brain tissues to allow for multisite neuronal light-activation.[93] Alternatively, various ways of patterned illumination have been developed for differential light activation in a sample.[94]

Gene delivery systems, such as viruses are currently been used to deliver opsins to select neuronal populations. Examples of such vectors include herpes, rabies and adeno- and lenti-associated viruses, with the latter two being the most commonly used.[95] For example, Boyden et al. transfected cultured neurons with lentiviruses bearing the ChR2 protein tagged with a yellow fluorescent protein.[89] Adeno-associated viruses are small, nonpathogenic and replication-defective parvoviruses with single-stranded DNA genome. Multiple subtypes exist; for instance, AAV2 in particular has been shown to have high transduction efficiency in neurons while AAV9 has been used to deliver the *cop4* gene, which encodes the ChR2 protein, into rat ventricular cardiomyocytes *in vivo*.[94–96]. Additional delivery systems include the use of transgenes and the Cre/*loxP* recombination systems, as mentioned above, to target photoactivation of specific neural populations. In this system, *loxP* cassettes flank the *cop4* gene with a reporter gene encoding fluorescent protein and the Cre driver

expressing Cre recombinase under the control of a cell-specific promoter such as tyrosine hydroxylase or choline acetyltransferase.[35,97,98]

The initial application of optogenetics to cardiovascular research was in 2010 to locate and control cardiac pacemaker cells in zebrafish and in embryonic stem cell-derived cardiomyocytes in mice, and several studies have since been published regarding optogenetic control of cardiomyocytes.[99–105] Wang et al. have been able to demonstrate that optogenetic stimulation of noradrenergic neurons in the locus cereleus of the brain inhibits parasympathetic cardiac vagal neuron outflow that results in tachycardia.[35] Their group have further evaluated the neural axis in the murine heart by identifying and stimulating a subpopulation of cardiomyocytes that bear the *phenylethanolamine n-methyltransferase* gene, which encodes the enzyme that converts norepinephrine to epinephrine, to exert control on heart rhythm through the use of optogenetics.[106] Wengrowski et al. have shown photoactivation of cardiac sympathetic nerves affects cardiac electrical properties to increase heart rate along with cardiac contractile force (Figure 8).[97] To study the effects of vagal tone on exercise capacity, Machhada et al. utilized a viral vector system to target neurons in the rat brainstem dorsal ventral motor nucleus, the main vagal nucleus in the central nervous system, with channelrhodopsin ChIEF.[107] Activation of the dorsal ventral motor nucleus neurons resulted in increased cardiac contractility and exercise capacity. In sum, modern viral-based as well as Cre transgenic approaches, have been used to map the structural and functional properties of the autonomic nervous system controlling the heart.

Clinical Neuroimaging

Imaging techniques of myocardial innervation, although limited, do allow for the study of innervation in animal studies and living humans. [^{14}C]2-deoxyglucose has been used to radiolabel neurons in culture and *in vivo* in sympathetic ganglia in canine with neural uptake induced by stimulation and imaged using autoradiography.[108,109] C-11 hydroxyephedrine or radioiodinated metaiodobenzylguanidine (*m*IBG), which are catecholamine analogues that are taken up by sympathetic nerve terminals, can be used to visualize sympathetic innervation to the heart *in vivo* in dogs and humans using a gamma camera and positron emission tomography, respectively.[110–115] Bravo et al. used three different C-11 labeled catecholamines to identify neurotransmitter metabolites involved in vesicular storage, transport and degradation in the sympathetic nerve terminal and outlined the dynamic regeneration process of sympathetic nerve function in the transplanted heart.[116] In studies of *m*IBG, the radiotracer is injected and the mean counts per pixel in the heart are compared to those of the mediastinum to generate a heart/mediastinal (H/M) uptake ratio. Quantification of the H/M ratio has resulted in the identification of cutoffs that have been associated with disease progression and response to therapy.[117–124] In short, cardiac imaging employing radiotracers of sympathetic output to the heart has diagnostic and prognostic implications in heart failure and arrhythmic and ischemic heart disease that warrants further study.

Summary and Future Directions

The functional anatomy of the cardiac nervous system is complex. Early studies focused on describing the anatomy of the cardiac nervous system to help elucidate the role of the ANS in regional cardiac control. Concepts regarding cardiac neural control have been revised in

recent years with new physiological data and have created a new and exciting framework for understanding regulatory control of the mammalian heart. Direct single neural and network recordings from intrinsic cardiac and extra-cardiac ganglia provide the methods to study organ level physiology and a proper framework for interpretation.[27,125,126] The field is now poised from a clinical and instrumentation front to take full advantage of the cellular and molecular work that has been done in the past to probe autonomic circuits.

More recently, technological advances in optical mapping and optogenetics hold the promise of functionally mapping the specificities of cardiac neural innervation to understand the role that the autonomic nervous system plays in the pathophysiology of cardiovascular disease, with particular regard to therapeutically targeting select neural elements therein. As such, further discoveries in this arena hold the promise of developing neuroscience-based cardiovascular therapeutics in the future.

Acknowledgments

None.

FUNDING: This work is supported by National Institutes of Health (NIH)/National Heart, Lung, and Blood Institute (NHLBI) Grant HL127974-02 to P.S.R; NIH/NHLBI HL125730-03 to O.A.A.; NIH Stimulating Peripheral Activity to Relieve Conditions (SPARC) Grant 5U18EB021799 to J.L.A.; and NIH/NHLBI HL084261 & NIH SPARC Grant OT2OD023848 to K.S.

References

1. Jänig, W. Integrative Action of the Autonomic Nervous System: Neurobiology of Homeostasis. Cambridge University Press; 2008.
2. Barron HV, Lesh MD. Autonomic nervous system and sudden cardiac death. J. Am. Coll. Cardiol. 1996; 27:1053–1060. [PubMed: 8609321]
3. Nolan J, et al. Prospective study of heart rate variability and mortality in chronic heart failure: results of the United Kingdom heart failure evaluation and assessment of risk trial (UK-heart). Circulation. 1998; 98:1510–1516. [PubMed: 9769304]
4. La Rovere MT, Bigger JT, Marcus FI, Mortara A, Schwartz PJ. Baroreflex sensitivity and heart-rate variability in prediction of total cardiac mortality after myocardial infarction. ATRAMI (Autonomic Tone and Reflexes After Myocardial Infarction) Investigators. Lancet Lond. Engl. 1998; 351:478–484.
5. Floras JS. Sympathetic activation in human heart failure: diverse mechanisms, therapeutic opportunities. Acta Physiol. Scand. 2003; 177:391–398. [PubMed: 12609011]
6. Shen MJ, Zipes DP. Role of the autonomic nervous system in modulating cardiac arrhythmias. Circ. Res. 2014; 114:1004–1021. [PubMed: 24625726]
7. Beaumont E, et al. Vagus nerve stimulation mitigates intrinsic cardiac neuronal and adverse myocyte remodeling postmyocardial infarction. Am. J. Physiol. Heart Circ. Physiol. 2015; 309:H1198–1206. [PubMed: 26276818]
8. Shen MJ, Zipes DP. Interventional and device-based autonomic modulation in heart failure. Heart Fail. Clin. 2015; 11:337–348. [PubMed: 25834979]
9. Schwartz PJ. Cardiac sympathetic denervation to prevent life-threatening arrhythmias. Nat. Rev. Cardiol. 2014; 11:346–353. [PubMed: 24614115]
10. Shivkumar K, et al. Clinical neurocardiology defining the value of neuroscience-based cardiovascular therapeutics. J. Physiol. 2016; 594:3911–3954. [PubMed: 27114333]
11. Bourke T, et al. Neuraxial modulation for refractory ventricular arrhythmias: value of thoracic epidural anesthesia and surgical left cardiac sympathetic denervation. Circulation. 2010; 121:2255–2262. [PubMed: 20479150]

12. Kuntz A, Morehouse A. Thoracic sympathetic cardiac nerves in man: Their relation to cervical sympathetic ganglionectomy. Arch. Surg. 1930; 20:607–613.
13. Saccomanno G. The components of the upper thoracic sympathetic nerves. J. Comp. Neurol. 1943; 79:355–378.
14. Mizeres NJ. The cardiac plexus in man. Am. J. Anat. 1963; 112:141–151.
15. Randall WC, Armour JA, Geis WP, Lippincott DB. Regional cardiac distribution of the sympathetic nerves. Fed. Proc. 1972; 31:1199–1208. [PubMed: 5038369]
16. Hopkins DA, Armour JA. Localization of sympathetic postganglionic and parasympathetic preganglionic neurons which innervate different regions of the dog heart. J. Comp. Neurol. 1984; 229:186–198. [PubMed: 6501600]
17. Janes RD, et al. Anatomy of human extrinsic cardiac nerves and ganglia. Am. J. Cardiol. 1986; 57:299–309. [PubMed: 3946219]
18. Kawashima T. The autonomic nervous system of the human heart with special reference to its origin, course, and peripheral distribution. Anat. Embryol. (Berl.). 2005; 209:425–438. [PubMed: 15887046]
19. Standish A, Enquist LW, Schwaber JS. Innervation of the heart and its central medullary origin defined by viral tracing. Science. 1994; 263:232–234. [PubMed: 8284675]
20. Standish A, Enquist LW, Escardo JA, Schwaber JS. Central neuronal circuit innervating the rat heart defined by transneuronal transport of pseudorabies virus. J. Neurosci. Off. J. Soc. Neurosci. 1995; 15:1998–2012.
21. Hopkins DA, Bieger D, deVente J, Steinbusch WM. Vagal efferent projections: viscerotopy, neurochemistry and effects of vagotomy. Prog. Brain Res. 1996; 107:79–96. [PubMed: 8782514]
22. Ardell JL, Rajendran PS, Nier HA, KenKnight BH, Armour JA. Central-peripheral neural network interactions evoked by vagus nerve stimulation: functional consequences on control of cardiac function. Am. J. Physiol. Heart Circ. Physiol. 2015; 309:H1740–1752. [PubMed: 26371171]
23. Randall WC, Ardell JL. Selective parasympathectomy of automatic and conductile tissues of the canine heart. Am. J. Physiol. 1985; 248:H61–68. [PubMed: 3970176]
24. Yuan BX, Ardell JL, Hopkins DA, Losier AM, Armour JA. Gross and microscopic anatomy of the canine intrinsic cardiac nervous system. Anat. Rec. 1994; 239:75–87. [PubMed: 8037379]
25. Armour JA, Murphy DA, Yuan BX, Macdonald S, Hopkins DA. Gross and microscopic anatomy of the human intrinsic cardiac nervous system. Anat. Rec. 1997; 247:289–298. [PubMed: 9026008]
26. McFarland J, Anders A. The morbid Histology of the cardiac nervous Ganglia. J. Med. Res. 1913; 27:425–435. [PubMed: 19972092]
27. Armour JA. Potential clinical relevance of the ‘little brain’ on the mammalian heart. Exp. Physiol. 2008; 93:165–176. [PubMed: 17981929]
28. Pickel VM, Joh TH, Field PM, Becker CG, Reis DJ. Cellular localization of tyrosine hydroxylase by immunohistochemistry. J. Histochem. Cytochem. Off. J. Histochem. Soc. 1975; 23:1–12.
29. Todo K, et al. Origins of vagal preganglionic fibers to the sino-atrial and atrio-ventricular node regions in the cat heart as studied by the horseradish peroxidase method. Brain Res. 1977; 130:545–550. [PubMed: 890451]
30. Mesulam MM. Tetramethyl benzidine for horseradish peroxidase neurohistochemistry: a non-carcinogenic blue reaction product with superior sensitivity for visualizing neural afferents and efferents. J. Histochem. Cytochem. Off. J. Histochem. Soc. 1978; 26:106–117.
31. Oldfield BJ, McLachlan EM. Localization of sensory neurons traversing the stellate ganglion of the cat. J. Comp. Neurol. 1978; 182:915–922. [PubMed: 730853]
32. Kalia M, Mesulam MM. Brain stem projections of sensory and motor components of the vagus complex in the cat: II. Laryngeal, tracheobronchial, pulmonary, cardiac, and gastrointestinal branches. J. Comp. Neurol. 1980; 193:467–508. [PubMed: 7440778]
33. Hopkins DA, Armour JA. Ganglionic distribution of afferent neurons innervating the canine heart and cardiopulmonary nerves. J. Auton. Nerv. Syst. 1989; 26:213–222. [PubMed: 2754177]
34. Mendelowitz D, Kunze DL. Identification and dissociation of cardiovascular neurons from the medulla for patch clamp analysis. Neurosci. Lett. 1991; 132:217–221. [PubMed: 1784423]

35. Wang X, Piñol RA, Byrne P, Mendelowitz D. Optogenetic stimulation of locus ceruleus neurons augments inhibitory transmission to parasympathetic cardiac vagal neurons via activation of brainstem α1 and β1 receptors. J. Neurosci. Off. J. Soc. Neurosci. 2014; 34:6182–6189.
36. Kuypers HG, Bentivoglio M, van der Kooy D, Catsman-Berrevoets CE. Retrograde transport of bisbenzimide and propidium iodide through axons to their parent cell bodies. Neurosci. Lett. 1979; 12:1–7. [PubMed: 88694]
37. Bentivoglio M, Kuypers HG, Catsman-Berrevoets CE, Loewe H, Dann O. Two new fluorescent retrograde neuronal tracers which are transported over long distances. Neurosci. Lett. 1980; 18:25–30. [PubMed: 6189013]
38. Tomney PA, Hopkins DA, Armour JA. Axonal branching of canine sympathetic postganglionic cardiopulmonary neurons. A retrograde fluorescent labeling study. Brain Res. Bull. 1985; 14:443–452. [PubMed: 2411359]
39. Grkovic I, Fernandez K, McAllen RM, Anderson CR. Misidentification of cardiac vagal pre-ganglionic neurons after injections of retrograde tracer into the pericardial space in the rat. Cell Tissue Res. 2005; 321:335–340. [PubMed: 15995869]
40. DiFrancesco D, Tromba C. Inhibition of the hyperpolarization-activated current (if) induced by acetylcholine in rabbit sino-atrial node myocytes. J. Physiol. 1988; 405:477–491. [PubMed: 3255798]
41. Petit-Jacques J, Bois P, Bescond J, Lenfant J. Mechanism of muscarinic control of the high-threshold calcium current in rabbit sino-atrial node myocytes. Pflugers Arch. 1993; 423:21–27. [PubMed: 8387668]
42. Karnovsky MJ, Roots L. A 'DIRECT-COLORING' THIOCHOLINE METHOD FOR CHOLINESTERASES. J. Histochem. Cytochem. Off. J. Histochem. Soc. 1964; 12:219–221.
43. Tago H, Kimura H, Maeda T. Visualization of detailed acetylcholinesterase fiber and neuron staining in rat brain by a sensitive histochemical procedure. J. Histochem. Cytochem. Off. J. Histochem. Soc. 1986; 34:1431–1438.
44. Roberts LA, Slocum GR, Riley DA. Morphological study of the innervation pattern of the rabbit sinoatrial node. Am. J. Anat. 1989; 185:74–88. [PubMed: 2782278]
45. Wharton J, et al. Immunohistochemical demonstration of human cardiac innervation before and after transplantation. Circ. Res. 1990; 66:900–912. [PubMed: 2317894]
46. Batulevicius D, Pauziene N, Pauza DH. Architecture and age-related analysis of the neuronal number of the guinea pig intrinsic cardiac nerve plexus. Ann. Anat. Anat. Anz. Off. Organ Anat. Ges. 2005; 187:225–243.
47. Ulphani JS, et al. Quantitative analysis of parasympathetic innervation of the porcine heart. Heart Rhythm Off. J. Heart Rhythm Soc. 2010; 7:1113–1119.
48. Pauza DH, Pauziene N, Pakeltyte G, Stropus R. Comparative quantitative study of the intrinsic cardiac ganglia and neurons in the rat, guinea pig, dog and human as revealed by histochemical staining for acetylcholinesterase. Ann. Anat. Anat. Anz. Off. Organ Anat. Ges. 2002; 184:125–136.
49. Kawano H, Okada R, Yano K. Histological study on the distribution of autonomic nerves in the human heart. Heart Vessels. 2003; 18:32–39. [PubMed: 12644879]
50. Pauza DH, et al. A combined acetylcholinesterase and immunohistochemical method for precise anatomical analysis of intrinsic cardiac neural structures. Ann. Anat. Anat. Anz. Off. Organ Anat. Ges. 2014; 196:430–440.
51. Pauziene N, et al. Neuroanatomy of the pig cardiac ventricles. A stereomicroscopic, confocal and electron microscope study. Anat. Rec. Hoboken NJ 2007. 2017; doi: 10.1002/ar.23619
52. Schemann M, Sann H, Schaaf C, Mäder M. Identification of cholinergic neurons in enteric nervous system by antibodies against choline acetyltransferase. Am. J. Physiol. 1993; 265:G1005–1009. [PubMed: 8238509]
53. Mawe GM, Talmage EK, Lee KP, Parsons RL. Expression of choline acetyltransferase immunoreactivity in guinea pig cardiac ganglia. Cell Tissue Res. 1996; 285:281–286. [PubMed: 8766164]

54. Fedorov VV, Hucker WJ, Dobrzynski H, Rosenshtraukh LV, Efimov IR. Postganglionic nerve stimulation induces temporal inhibition of excitability in rabbit sinoatrial node. Am. J. Physiol. Heart Circ. Physiol. 2006; 291:H612–623. [PubMed: 16565321]
55. Hoover DB, Ganote CE, Ferguson SM, Blakely RD, Parsons RL. Localization of cholinergic innervation in guinea pig heart by immunohistochemistry for high-affinity choline transporters. Cardiovasc. Res. 2004; 62:112–121. [PubMed: 15023558]
56. Mabe AM, Hoard JL, Duffourc MM, Hoover DB. Localization of cholinergic innervation and neurturin receptors in adult mouse heart and expression of the neurturin gene. Cell Tissue Res. 2006; 326:57–67. [PubMed: 16708241]
57. Crick SJ, Anderson RH, Ho SY, Sheppard MN. Localisation and quantitation of autonomic innervation in the porcine heart II: endocardium, myocardium and epicardium. J. Anat. 1999; 195(Pt 3):359–373. [PubMed: 10580851]
58. Kreipke RE, Birren SJ. Innervating sympathetic neurons regulate heart size and the timing of cardiomyocyte cell cycle withdrawal. J. Physiol. 2015; 593:5057–5073. [PubMed: 26420487]
59. Khan IA, Ludueña RF. Phosphorylation of beta III-tubulin. Biochemistry (Mosc.). 1996; 35:3704–3711.
60. Mahmoud AI, et al. Nerves Regulate Cardiomyocyte Proliferation and Heart Regeneration. Dev. Cell. 2015; 34:387–399. [PubMed: 26256209]
61. White IA, Gordon J, Balkan W, Hare JM. Sympathetic Reinnervation Is Required for Mammalian Cardiac Regeneration. Circ. Res. 2015; 117:990–994. [PubMed: 26371181]
62. Hoard JL, et al. Cholinergic neurons of mouse intrinsic cardiac ganglia contain noradrenergic enzymes, norepinephrine transporters, and the neurotrophin receptors tropomyosin-related kinase A and p75. Neuroscience. 2008; 156:129–142. [PubMed: 18674600]
63. Gitler D, et al. Molecular determinants of synapsin targeting to presynaptic terminals. J. Neurosci. Off. J. Soc. Neurosci. 2004; 24:3711–3720.
64. Rysevaite K, et al. Immunohistochemical characterization of the intrinsic cardiac neural plexus in whole-mount mouse heart preparations. Heart Rhythm Off. J. Heart Rhythm Soc. 2011; 8:731–738.
65. Echelard Y, Vassileva G, McMahon AP. Cis-acting regulatory sequences governing Wnt-1 expression in the developing mouse CNS. Dev. Camb. Engl. 1994; 120:2213–2224.
66. Miller CE, et al. Confocal imaging of the embryonic heart: how deep? Microsc. Microanal. Off. J. Microsc. Soc. Am. Microbeam Anal. Soc. Microsc. Soc. Can. 2005; 11:216–223.
67. Becker K, Jährling N, Saghafi S, Weiler R, Dodt H-U. Chemical clearing and dehydration of GFP expressing mouse brains. PloS One. 2012; 7:e33916. [PubMed: 22479475]
68. Ertürk A, et al. Three-dimensional imaging of solvent-cleared organs using 3DISCO. Nat. Protoc. 2012; 7:1983–1995. [PubMed: 23060243]
69. Hama H, et al. Scale: a chemical approach for fluorescence imaging and reconstruction of transparent mouse brain. Nat. Neurosci. 2011; 14:1481–1488. [PubMed: 21878933]
70. Renier N, et al. iDISCO: a simple, rapid method to immunolabel large tissue samples for volume imaging. Cell. 2014; 159:896–910. [PubMed: 25417164]
71. Ke M-T, Fujimoto S, Imai T. SeeDB: a simple and morphology-preserving optical clearing agent for neuronal circuit reconstruction. Nat. Neurosci. 2013; 16:1154–1161. [PubMed: 23792946]
72. Tainaka K, et al. Whole-body imaging with single-cell resolution by tissue decolorization. Cell. 2014; 159:911–924. [PubMed: 25417165]
73. Kuwajima T, et al. ClearT: a detergent- and solvent-free clearing method for neuronal and non-neuronal tissue. Dev. Camb. Engl. 2013; 140:1364–1368.
74. Chung K, et al. Structural and molecular interrogation of intact biological systems. Nature. 2013; 497:332–337. [PubMed: 23575631]
75. Yang B, et al. Single-cell phenotyping within transparent intact tissue through whole-body clearing. Cell. 2014; 158:945–958. [PubMed: 25088144]
76. Ito M, Zipes DP. Efferent sympathetic and vagal innervation of the canine right ventricle. Circulation. 1994; 90:1459–1468. [PubMed: 8087953]

77. Chiou CW, Eble JN, Zipes DP. Efferent vagal innervation of the canine atria and sinus and atrioventricular nodes. The third fat pad. Circulation. 1997; 95:2573–2584. [PubMed: 9184589]
78. Ajijola OA, et al. Sympathetic Modulation of Electrical Activation In Normal and Infarcted Myocardium: Implications for Arrhythmogenesis. Am. J. Physiol. Heart Circ. Physiol. 2017; ajpheart.00575.2016. doi: 10.1152/ajpheart.00575.2016
79. Yamakawa K, et al. Vagal nerve stimulation activates vagal afferent fibers that reduce cardiac efferent parasympathetic effects. Am. J. Physiol. Heart Circ. Physiol. 2015; 309:H1579–1590. [PubMed: 26371172]
80. Norris JE, Foreman RD, Wurster RK. Responses of the canine heart to stimulation of the first five ventral thoracic roots. Am. J. Physiol. 1974; 227:9–12. [PubMed: 4843349]
81. Norris JE, Lippincott D, Wurster RD. Responses of canine endocardium to stimulation of the upper thoracic roots. Am. J. Physiol. 1977; 233:H655–659. [PubMed: 596462]
82. Cohn AE. On the differences in the effects of stimulation of the two vagus nerves on rate and conduction of the dog's heart. J. Exp. Med. 1912; 16:732–757. [PubMed: 19867609]
83. Levy MN, Zieske H. Autonomic control of cardiac pacemaker activity and atrioventricular transmission. J. Appl. Physiol. 1969; 27:465–470. [PubMed: 5822553]
84. Randall WC, Ardell JL, Becker DM. Differential responses accompanying sequential stimulation and ablation of vagal branches to dog heart. Am. J. Physiol. 1985; 249:H133–140. [PubMed: 4014479]
85. Loeb JM, deTarnowsky JM. Integration of heart rate and sympathetic neural effects on AV conduction. Am. J. Physiol. 1988; 254:H651–657. [PubMed: 3354694]
86. Ng GA, Brack KE, Coote JH. Effects of direct sympathetic and vagus nerve stimulation on the physiology of the whole heart--a novel model of isolated Langendorff perfused rabbit heart with intact dual autonomic innervation. Exp. Physiol. 2001; 86:319–329. [PubMed: 11471534]
87. Zemelman BV, Lee GA, Ng M, Miesenböck G. Selective photostimulation of genetically chARGed neurons. Neuron. 2002; 33:15–22. [PubMed: 11779476]
88. Nagel G, et al. Channelrhodopsin-2, a directly light-gated cation-selective membrane channel. Proc. Natl. Acad. Sci. U. S. A. 2003; 100:13940–13945. [PubMed: 14615590]
89. Boyden ES, Zhang F, Bamberg E, Nagel G, Deisseroth K. Millisecond-timescale, genetically targeted optical control of neural activity. Nat. Neurosci. 2005; 8:1263–1268. [PubMed: 16116447]
90. Berndt A, et al. High-efficiency channelrhodopsins for fast neuronal stimulation at low light levels. Proc. Natl. Acad. Sci. U. S. A. 2011; 108:7595–7600. [PubMed: 21504945]
91. Kleinlogel S, et al. Ultra light-sensitive and fast neuronal activation with the Ca^{2}+-permeable channelrhodopsin CatCh. Nat. Neurosci. 2011; 14:513–518. [PubMed: 21399632]
92. Lin JY, Lin MZ, Steinbach P, Tsien RY. Characterization of engineered channelrhodopsin variants with improved properties and kinetics. Biophys. J. 2009; 96:1803–1814. [PubMed: 19254539]
93. Stark E, Koos T, Buzsáki G. Diode probes for spatiotemporal optical control of multiple neurons in freely moving animals. J. Neurophysiol. 2012; 108:349–363. [PubMed: 22496529]
94. Packer AM, Roska B, Häusser M. Targeting neurons and photons for optogenetics. Nat. Neurosci. 2013; 16:805–815. [PubMed: 23799473]
95. Yizhar O, Fenno LE, Davidson TJ, Mogri M, Deisseroth K. Optogenetics in neural systems. Neuron. 2011; 71:9–34. [PubMed: 21745635]
96. Nussinovitch U, Gepstein L. Optogenetics for in vivo cardiac pacing and resynchronization therapies. Nat. Biotechnol. 2015; 33:750–754. [PubMed: 26098449]
97. Wengrowski AM, et al. Optogenetic release of norepinephrine from cardiac sympathetic neurons alters mechanical and electrical function. Cardiovasc. Res. 2015; 105:143–150. [PubMed: 25514932]
98. Kalmbach A, Hedrick T, Waters J. Selective optogenetic stimulation of cholinergic axons in neocortex. J. Neurophysiol. 2012; 107:2008–2019. [PubMed: 22236708]
99. Arrenberg AB, Stainier DYR, Baier H, Huisken J. Optogenetic control of cardiac function. Science. 2010; 330:971–974. [PubMed: 21071670]

100. Bruegmann T, et al. Optogenetic control of heart muscle in vitro and in vivo. Nat. Methods. 2010; 7:897–900. [PubMed: 20881965]
101. Jia Z, et al. Stimulating cardiac muscle by light: cardiac optogenetics by cell delivery. Circ. Arrhythm. Electrophysiol. 2011; 4:753–760. [PubMed: 21828312]
102. Boyle PM, Williams JC, Ambrosi CM, Entcheva E, Trayanova NA. A comprehensive multiscale framework for simulating optogenetics in the heart. Nat. Commun. 2013; 4:2370. [PubMed: 23982300]
103. Beiert T, Bruegmann T, Sasse P. Optogenetic activation of Gq signalling modulates pacemaker activity of cardiomyocytes. Cardiovasc. Res. 2014; 102:507–516. [PubMed: 24576953]
104. Bingen BO, et al. Light-induced termination of spiral wave arrhythmias by optogenetic engineering of atrial cardiomyocytes. Cardiovasc. Res. 2014; 104:194–205. [PubMed: 25082848]
105. Park SA, Lee S-R, Tung L, Yue DT. Optical mapping of optogenetically shaped cardiac action potentials. Sci. Rep. 2014; 4:6125. [PubMed: 25135113]
106. Wang Y, et al. Optogenetic Control of Heart Rhythm by Selective Stimulation of Cardiomyocytes Derived from Pnmt(+) Cells in Murine Heart. Sci. Rep. 2017; 7:40687. [PubMed: 28084430]
107. Machhada A, et al. Vagal determinants of exercise capacity. Nat. Commun. 2017; 8:15097. [PubMed: 28516907]
108. Saji M, Obata K. Stimulus-dependent labeling of cultured ganglionic cell with [14C]2-deoxyglucose. Brain Res. 1981; 212:435–446. [PubMed: 6112051]
109. Kostreva DR, Armour JA, Bosnjak ZJ. Metabolic mapping of a cardiac reflex mediated by sympathetic ganglia in dogs. Am. J. Physiol. 1985; 249:R317–322. [PubMed: 3929629]
110. Kline RC, et al. Myocardial imaging in man with I-123 meta-iodobenzylguanidine. J. Nucl. Med. Off. Publ. Soc. Nucl. Med. 1981; 22:129–132.
111. Wieland DM, et al. Myocardial imaging with a radioiodinated norepinephrine storage analog. J. Nucl. Med. Off. Publ. Soc. Nucl. Med. 1981; 22:22–31.
112. Sisson JC, et al. Scintigraphic detection of regional disruption of adrenergic neurons in the heart. Am. Heart J. 1988; 116:67–76. [PubMed: 3394634]
113. Dae MW, et al. Scintigraphic assessment of regional cardiac adrenergic innervation. Circulation. 1989; 79:634–644. [PubMed: 2783894]
114. Schwaiger M, et al. Noninvasive evaluation of sympathetic nervous system in human heart by positron emission tomography. Circulation. 1990; 82:457–464. [PubMed: 2372893]
115. Calkins H, Lehmann MH, Allman K, Wieland D, Schwaiger M. Scintigraphic pattern of regional cardiac sympathetic innervation in patients with familial long QT syndrome using positron emission tomography. Circulation. 1993; 87:1616–1621. [PubMed: 8491017]
116. Bravo PE, et al. Mechanistic Insights into Sympathetic Neuronal Regeneration: Multitracer Molecular Imaging of Catecholamine Handling After Cardiac Transplantation. Circ. Cardiovasc. Imaging. 2015; 8:e003507. [PubMed: 26245765]
117. Jacobson AF, et al. Myocardial iodine-123 meta-iodobenzylguanidine imaging and cardiac events in heart failure. Results of the prospective ADMIRE-HF (AdreView Myocardial Imaging for Risk Evaluation in Heart Failure) study. J. Am. Coll. Cardiol. 2010; 55:2212–2221. [PubMed: 20188504]
118. Gerson MC, et al. Carvedilol improves left ventricular function in heart failure patients with idiopathic dilated cardiomyopathy and a wide range of sympathetic nervous system function as measured by iodine 123 metaiodobenzylguanidine. J. Nucl. Cardiol. Off. Publ. Am. Soc. Nucl. Cardiol. 2002; 9:608–615.
119. Toyama T, et al. Cardiac sympathetic activity estimated by 123I-MIBG myocardial imaging in patients with dilated cardiomyopathy after beta-blocker or angiotensin-converting enzyme inhibitor therapy. J. Nucl. Med. Off. Publ. Soc. Nucl. Med. 1999; 40:217–223.
120. Kasama S, et al. Effects of candesartan on cardiac sympathetic nerve activity in patients with congestive heart failure and preserved left ventricular ejection fraction. J. Am. Coll. Cardiol. 2005; 45:661–667. [PubMed: 15734608]
121. Somsen GA, et al. Increased myocardial [123I]-metaiodobenzylguanidine uptake after enalapril treatment in patients with chronic heart failure. Heart Br. Card. Soc. 1996; 76:218–222.

122. Kasama S, et al. Spironolactone improves cardiac sympathetic nerve activity and symptoms in patients with congestive heart failure. J. Nucl. Med. Off. Publ. Soc. Nucl. Med. 2002; 43:1279–1285.

123. Nagahara D, et al. Predicting the need for an implantable cardioverter defibrillator using cardiac metaiodobenzylguanidine activity together with plasma natriuretic peptide concentration or left ventricular function. J. Nucl. Med. Off. Publ. Soc. Nucl. Med. 2008; 49:225–233.

124. Tomoda H, et al. Regional sympathetic denervation detected by iodine 123 metaiodobenzylguanidine in non-Q-wave myocardial infarction and unstable angina. Am. Heart J. 1994; 128:452–458. [PubMed: 8074004]

125. Armour JA. Cardiac neuronal hierarchy in health and disease. Am. J. Physiol. Regul. Integr. Comp. Physiol. 2004; 287:R262–271. [PubMed: 15271675]

126. Beaumont E, et al. Network interactions within the canine intrinsic cardiac nervous system: implications for reflex control of regional cardiac function. J. Physiol. 2013; 591:4515–4533. [PubMed: 23818689]

127. Jänig W. Neurocardiology: a neurobiologist's perspective. J. Physiol. 2016; 594:3955–3962. [PubMed: 27417671]

128. Dilsizian, V., Narula, J. Atlas of Cardiac Innervation. Springer International Publishing; 2017.

129. Hoover DB, et al. Localization of multiple neurotransmitters in surgically derived specimens of human atrial ganglia. Neuroscience. 2009; 164:1170–1179. [PubMed: 19747529]

130. Ajijola OA, et al. Focal myocardial infarction induces global remodeling of cardiac sympathetic innervation: neural remodeling in a spatial context. Am. J. Physiol. Heart Circ. Physiol. 2013; 305:H1031–1040. [PubMed: 23893167]

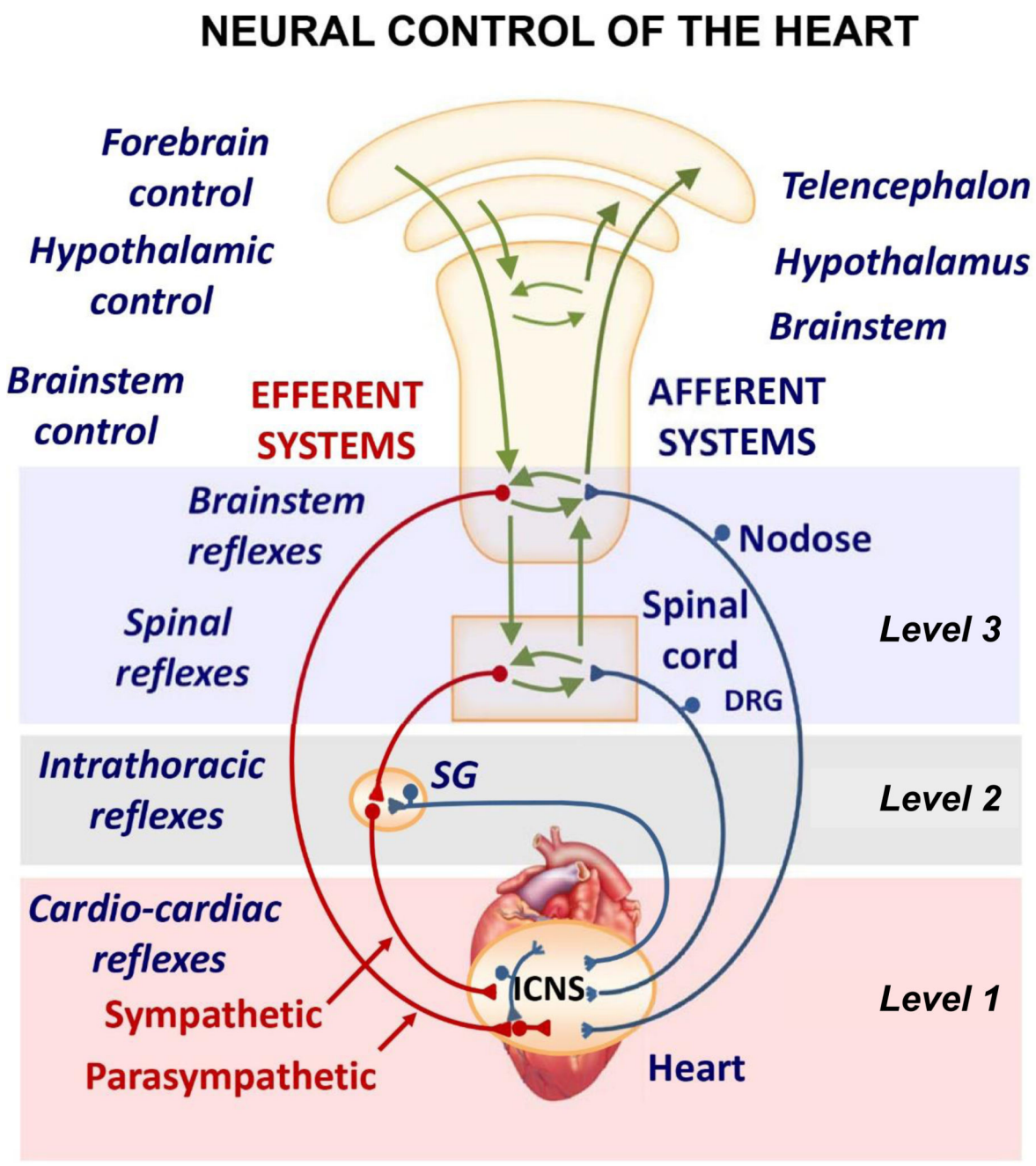

Figure 1.

Neural control of the heart. Autonomic control of the heart is comprised of a series of nested feedback loops, from the intracardiac neurons (level 1) to the intrathoracic extra-cardiac neurons (levels 2) and the central nervous system (level 3). SG, sympathetic ganglion; DRG, dorsal root ganglion; ICNS, intracardiac nervous system. Adapted from *Janig*.[127]

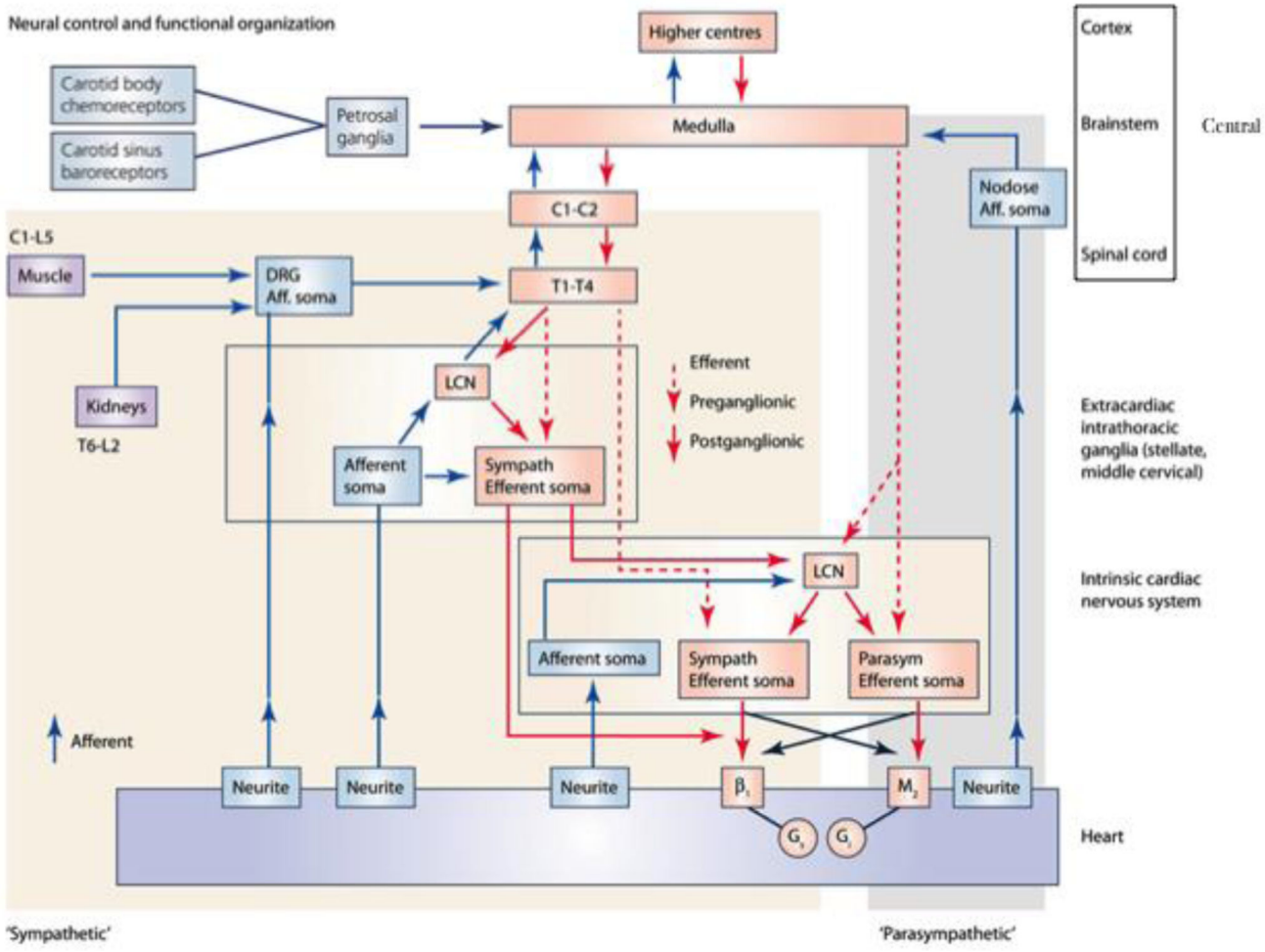

Figure 2.

Neurohumoral control and functional organization of cardiac innervation. Aff, afferent; β_1, β-adrenergic receptor; C, cervical; DRG, dorsal root ganglion; G_i, inhibitory G-protein; G_s, stimulatory G-protein; L, lumbar; LCN, local circuit neuron; M_2, muscarinic receptor; T, thoracic. Adapted from *Shivkumar et al.*[10]

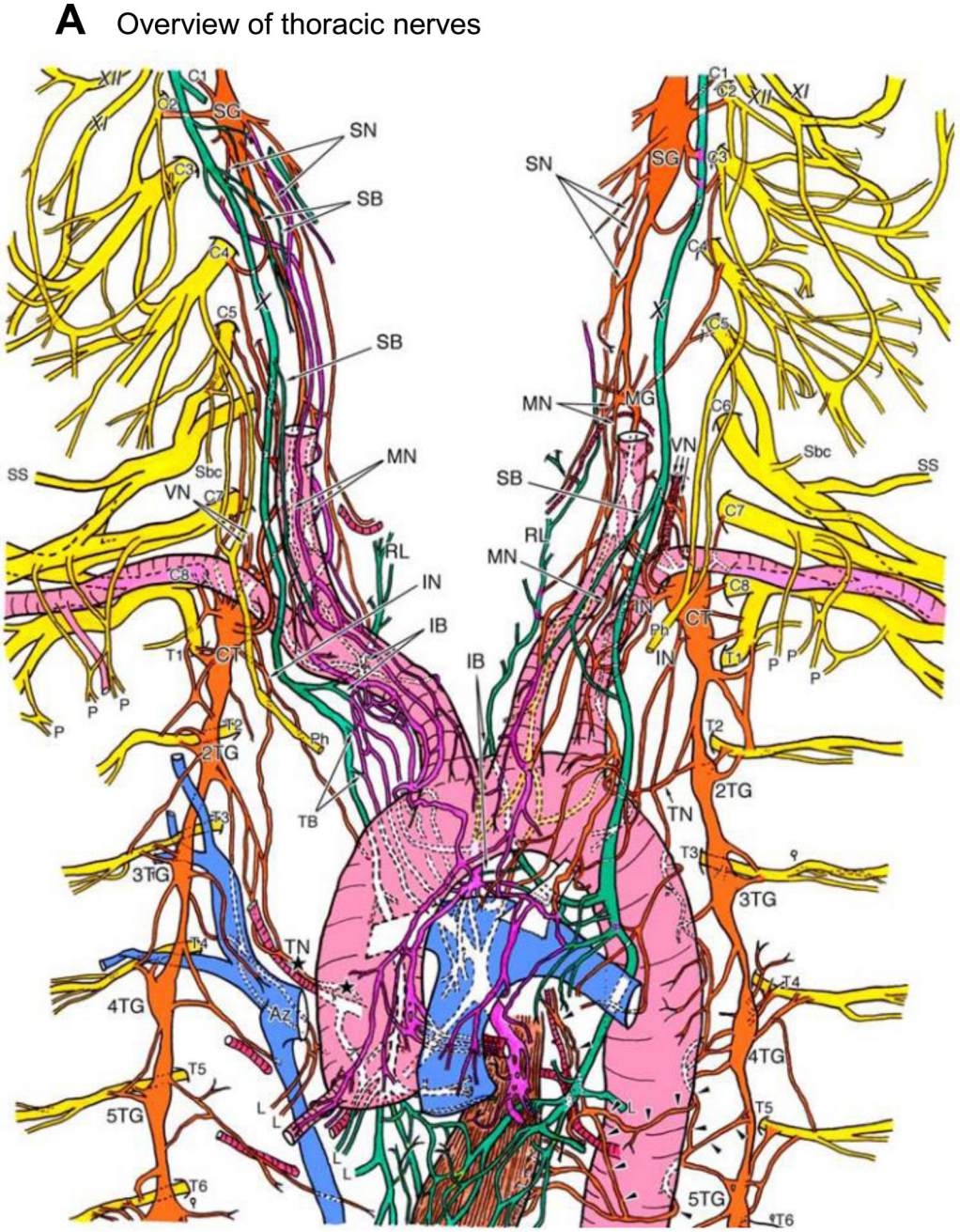

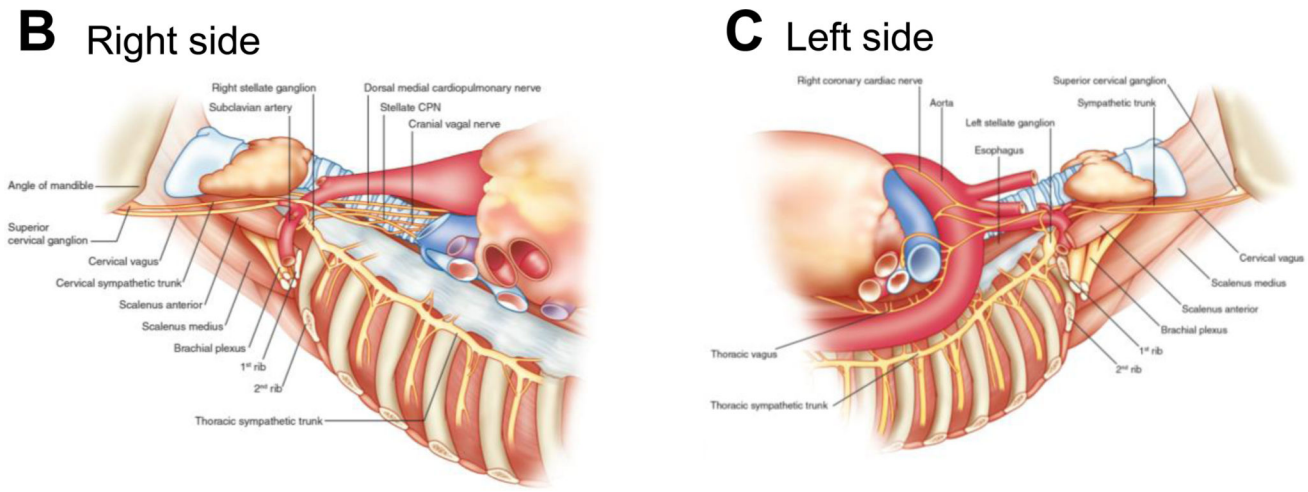

Figure 3.

A, Detailed illustration of the course of the autonomic cardiac nerves. The innervation of the heart via the right thoracic cardiac nerve and the inferior cardiac nerve is shown by the black stars. The arrowheads highlight the course of the left thoracic cardiac nerve. The sympathetic cardiac nerves, vagal cardiac branches, and the cardiac plexuses are colored in orange, green and purple, respectively. AI, anterior interventricular branch; Ao, aorta; Az, azygos vein; CB, circumflex branch; CC, common carotid artery; CT, cervicothoracic (stellate) ganglion; GV, great cardiac vein; IB, inferior (vagal) cardiac branch; IG, inferior cervical ganglion; IN, inferior cervical cardiac nerve; L, lung; LA, left atrium; LCA, left coronary artery; MG, middle cervical ganglion; MN, middle cardiac nerve; P, pectoral nerve; Ph, phrenic nerve; PT, pulmonary trunk; RA, right atrium; RCA, right coronary artery; RL, recurrent laryngeal nerve of vagus nerve; SB, superior (vagal) cardiac branch; Sbc, nerve to subclavian muscle; SG, superior cervical ganglion; SN, superior cardiac nerve; SS, suprascapular nerve; SVC, superior vena cava; TB, thoracic (vagal) cardiac branch; TG, thoracic ganglia; TN, thoracic cardiac nerve; VG, vertebral ganglion; VN, vertebral nerve; X, vagus nerve; XI, accessory nerve; XII, hypoglossal nerve. Adapted from *Kawashima*.[18] Course of the right (B) and left (C) sympathetic trunks, vagus nerve and their major branches in an embalmed cadaver. Adapted from *Janes et al*. and *Dilsizian and Narula*.[17,128]

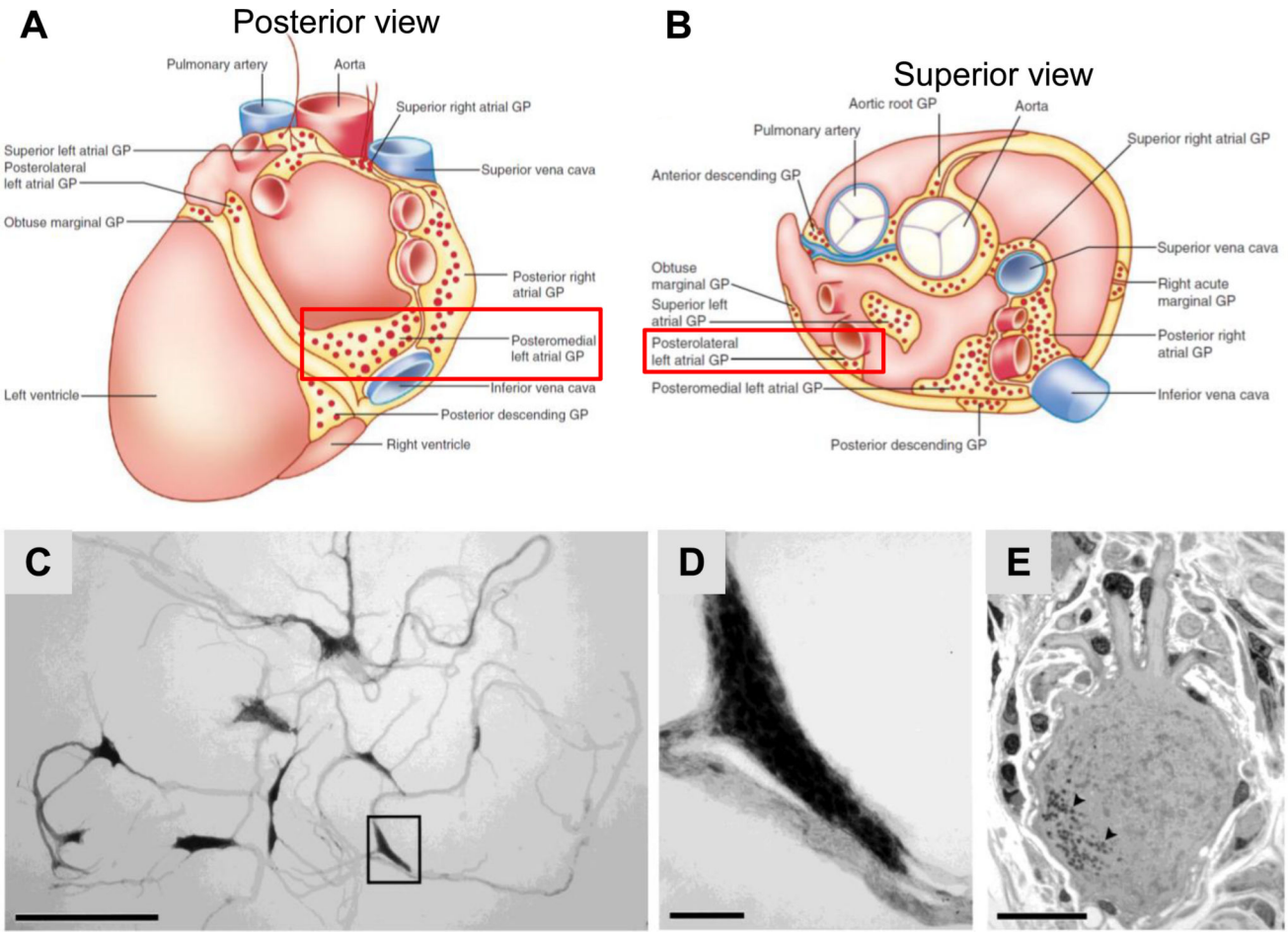

Figure 4.

A–B, Distribution of the intrinsic cardiac ganglionated plexuses (GP) in the heart. A, posterior; B, superior. Adapted from *Dilsizian and Narula*.[128] C–E, Light photomicrographs of human intrinsic cardiac nerves, ganglia and neurons. C, Network of ganglia and nerves stained with methylene blue and dissected from the posteromedial left atrial ganglionated plexus. The ganglia appear as expansions along a nerve (box). D, Enlargement of boxed area in A illustrating a ganglion composed of approximately 150–200 nerve cell bodies. E, High-magnification micrograph of a multipolar neuron. Note the accumulation of lipofuscin granules (arrowheads). Scale bars 52.5mm in C, 250μm in D, 25μm in E. Adapted from *Armour et al*.[25]

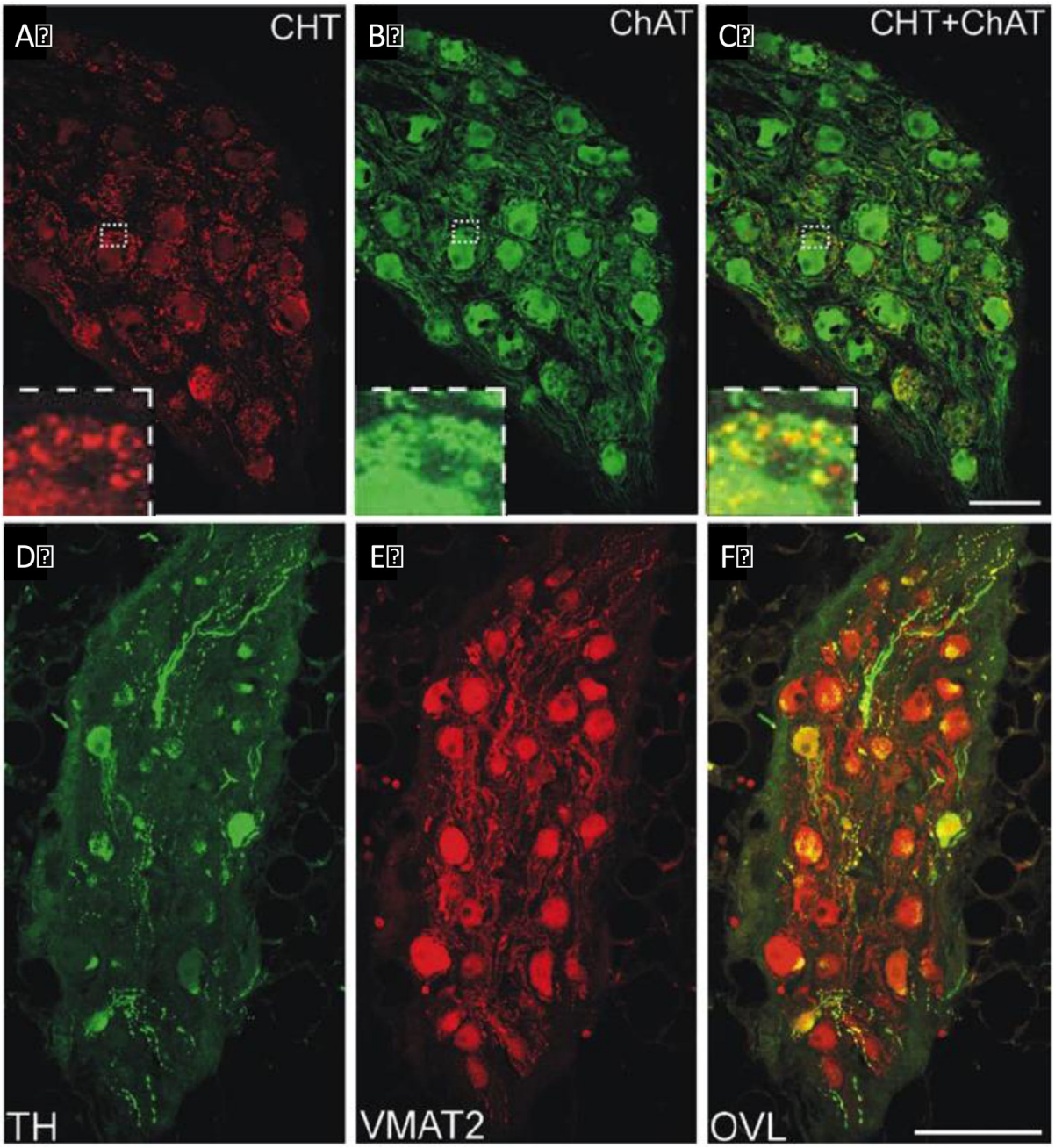

Figure 5.

Confocal images of human intrinsic cardiac neurons expressing the cholinergic and adrenergic phenotypes. A–C, Confocal images of a ganglion that was double labeled to show CHT (A) and ChAT (B). CHT immunoreactivity (A, red) was prominent in varicose nerve fibers around intrinsic cardiac neurons and faint or absent in the neuronal cell bodies. In contrast, staining for ChAT (B, green) was notable in neuronal cell bodies and generally less intense in surrounding nerve processes. (C) Colocalization of CHT and ChAT (yellow) was noted in some cell bodies and nerve processes in the overlay image (CHT+ChAT). Inserts at lower left show boxed areas at higher magnification. All panels contain maximum projection

images compiled from confocal scans that spanned 8μm. Scale bar = 100μm in A–C. D–F Confocal images of a section that was double labeled to show TH (D, green) and VMAT2 (E, red). (D) Few neurons and nerve fibers stained for TH. (B) Prominent staining for VMAT2 occurred in most neurons and many nerves fibers. (C) Overlap (OVL) of TH and VMAT2 images shows that a significant amount of the TH colocalizes (yellow) with VMAT2. All panels contain maximum projection images compiled from confocal scans that spanned 10μm. Scale bar = 150μm. Adapted from *Hoover et al.*[129]

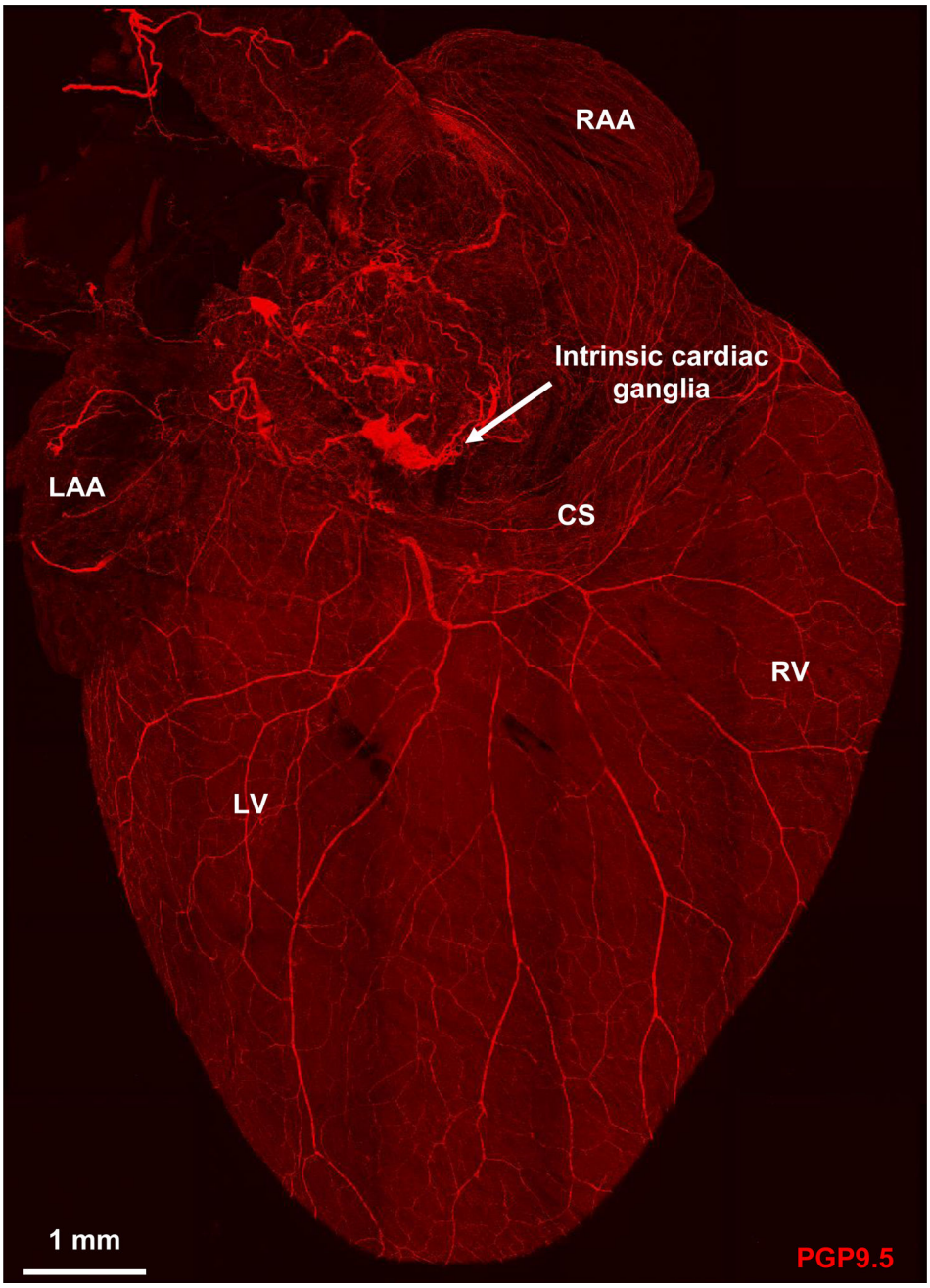

Figure 6.

Confocal image of dorsal surface of mouse heart stained with pan-neuronal marker protein gene product 9.5 (PGP9.5) and demonstrating the rich innervation of the heart. CS, coronary sinus; LAA, left atrial appendage; LV, left ventricle; RAA, right atrial appendage; RV, right ventricle.

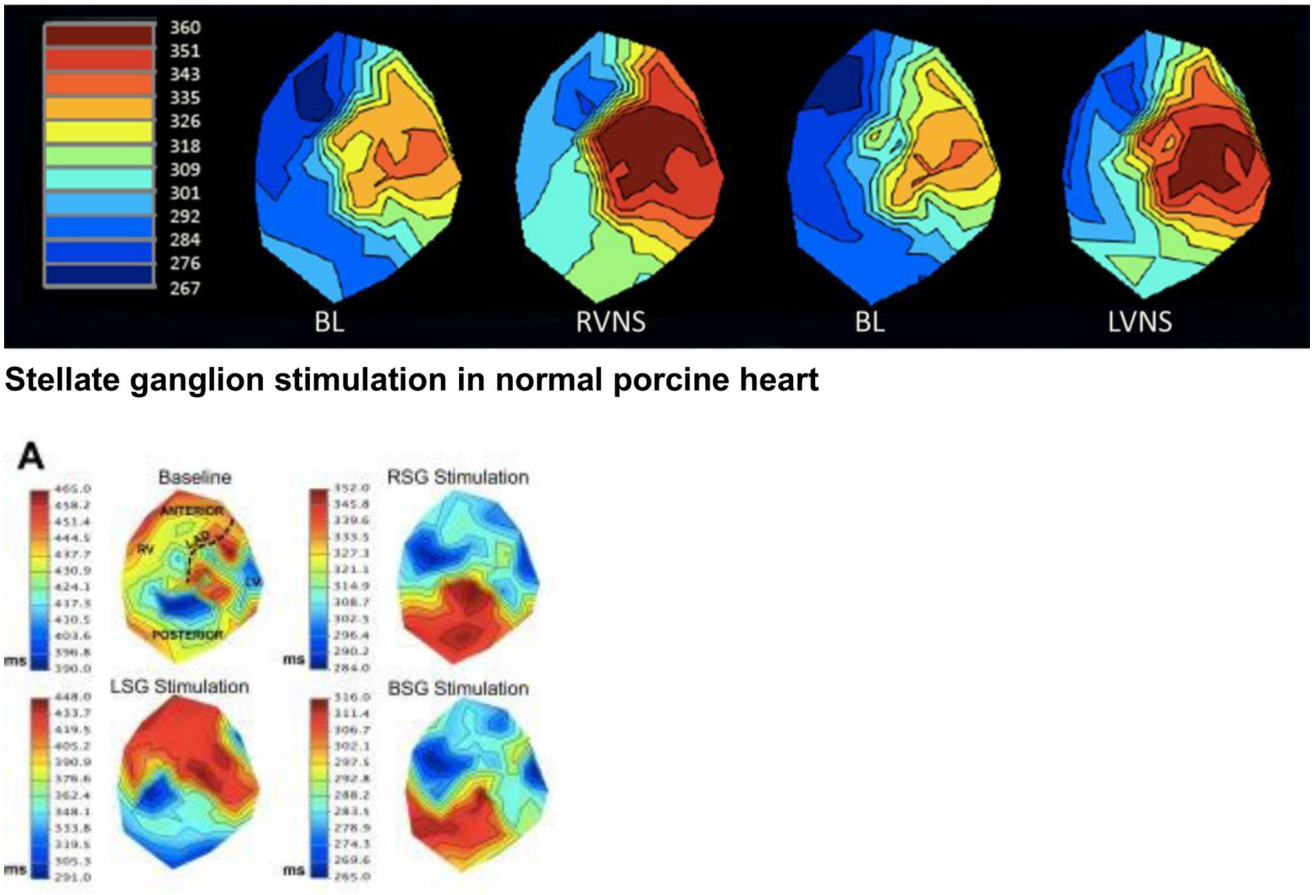

Figure 7.

A, Activation recovery interval (ARI) maps at baseline and during right (RVNS) and left (LVNS) vagal nerve stimulation in a normal porcine heart. No significant regional differences in responses were found. Adapted from *Yamakawa et al.*[79] B, ARI maps in control porcine hearts at baseline (BL) and during right (RSG), left (LSG) and bilateral (BSG) stellate ganglion stimulation. Myocardial regions are displayed in the BL control map. Adapted from *Ajijola et al.*[130]

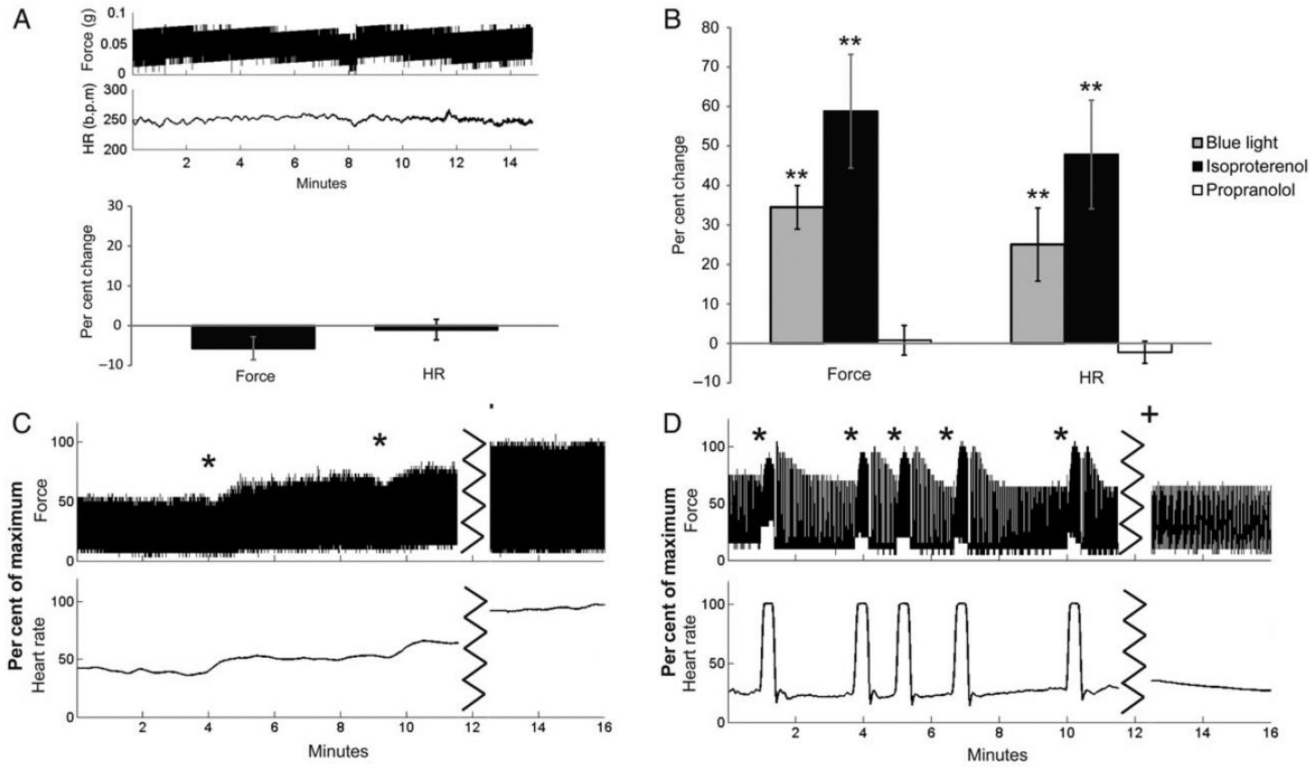

Effects of blue light photostimulation on heart rate and contractile force in Langendorff-perfused mouse hearts. A, Stability of force and heart rate shown over 15 minutes (top) and expressed as percent change (bottom, n = 8). B, Percent change from control phase after stimulating with blue light (grey, n = 10), administering isoproterenol (black, n = 5), or stimulating with blue light after administering propranolol (white, n = 5). C, Changes in force and heart rate after two rounds of blue light photostimulation (*) and addition of isoproterenol (+). D, Changes in force and heart rate after several rounds of blue light photostimulation (*) and response to photostimulation after administration of propranolol (+). **P<0.05 statistically different form baseline. Adapted from *Wengrowski et al.*[97]